Development 133, 3597-3606 (2006) doi:10.1242/dev.02534

Deleted in cancer 1 (DICE1) is an essential protein controlling the topology of the inner mitochondrial membrane in *C. elegans*

Sung Min Han[1,*], Tae Hoon Lee[1,*], Ji Young Mun[2,*], Moon Jeong Kim[1], Ekaterini A. Kritikou[3], Se-Jin Lee[1], Sung Sik Han[2], Michael O. Hengartner[3] and Hyeon-Sook Koo[1,†]

DICE1 (deleted in cancer 1), first identified in human lung carcinoma cell lines, is a candidate tumor suppressor, but the details of its activity remain largely unknown. We have found that RNA interference of its *C. elegans* homolog (DIC-1) produced inviable embryos with increased apoptosis, cavities in cells and abnormal morphogenesis. In the *dic-1*(RNA*i*) germ line, *ced-3*-dependent apoptosis increased, and cell cavities appeared at the late-pachytene/oogenic stage, leading to defective oogenesis. Immunofluorescence microscopy of DIC-1 revealed its ubiquitous expression in the form of cytoplasmic foci, and cryoelectron microscopy narrowed down the location of the foci to the inner membrane of mitochondria. After *dic-1* RNA*i*, mitochondria had an irregular morphology and contained numerous internal vesicles. Homozygous embryos from a heterozygous *dic-1* mother arrested at the L3 larval stage, in agreement with the essential role of DIC-1 in mitochondria. In summary, *C. elegans* DIC-1 plays a crucial role in the formation of normal morphology of the mitochondrial cristae/inner membrane. Our results suggest that human DICE1 may have several functions in multiple intracellular locations.

KEY WORDS: DICE1 (INTS6), Apoptosis, Mitochondria, Cristae remodeling, *C. elegans*

INTRODUCTION

DICE1 (deleted in cancer 1; INTS6 – Human Gene Nomenclature Database) was originally isolated as a gene responsible for non-small cell lung carcinoma resulting from loss of heterozygosity in human chromosome 13q14 (Wieland et al., 1999). Although *DICE1* mRNA was detected in all human tissues, it was downregulated or absent in cell lines and tissues of non-small cell lung carcinoma. Hypermethylation of its promoter region was associated with its downregulation in several cell lines derived from non-small cell carcinomas (Wieland et al., 2001) and prostate cancers (Röpke et al., 2005). Ectopic expression of DICE1 inhibited colony formation by cell lines of both non-small cell lung cancer and prostate cancer, and suppressed anchorage-independent growth of mouse fibroblasts transformed with the IGF1 receptor gene (Wieland et al., 2004). Overexpression of a mouse DICE1 homolog (DBI1) also suppressed induction of cell proliferation by IGF1 (Hoff et al., 1998). DBI1 was located in the nuclear fraction (Hoff et al., 1998), in agreement with the nuclear localization of EGFP-tagged human DICE1 in COS cells (Wieland et al., 2001).

Although DICE1 homologs in humans and mice are thought to be suppressors of cell proliferation, the mode of action of the proteins is largely unknown, because they contain only one functional domain, as defined by current prediction algorithms: the N terminus of each DICE1 homolog has a conserved amino acid sequence encoding a von Willebrand factor type A domain (VWF A) (Fig. 1). This domain is known to be involved in cell-cell, cell-extracellular matrix and intracellular protein-protein interactions, as observed in more than 20 human proteins, including the von Willebrand blood clotting factor, some types of collagens, integrin subunits and leukocyte adhesion receptor (for reviews, see Colombatti and Bonaldo, 1991; Whittaker and Hynes, 2002). Although the presence of a DEAD-box in human DICE1 suggests a helicase function, no DEAD box is present in the *C. elegans* homolog, and a more extensive helicase motif is not found in any DICE1 homologs. The likelihood that DICE1 acts as a helicase is thus very low, and the conserved VWF A domain does not suggest any other potential role.

In this study, we set out to analyze the knockdown and knockout phenotypes of a *C. elegans* DICE1 homolog in order to elucidate the molecular function of human DICE1. The protein is essential for *C. elegans* oogenesis, late embryogenesis and larval growth, and its deficiency induces apoptosis. It is localized to the mitochondrial inner membrane, and abnormalities in both overall and inner mitochondrial morphologies result from its absence. The localization of DICE1 and the phenotypes caused by its deficiency suggest that it is involved in remodeling of the mitochondrial cristae in *C. elegans*. *C. elegans* DICE1 shows differences in its subcellular location and function from the human homolog, and our results imply either that they have distinct functions due to divergent evolution, or that the proteins have additional cryptic roles.

MATERIALS AND METHODS

Strains

Bristol N2, a standard wild-type strain, and *ced-1(e1735)*, *ced-3(n717)*, *ced-4(n1162)*, *cep-1(gk138)*, *elo-5(ok683)/nT1[qIs51]* and *ajm-1::gfp* (strain SU93) strains were obtained from the *Caenorhabditis* Genetics Center (Minneapolis, MN, USA) and maintained at 20°C according to standard procedures. *dic-1(tm1615)* was generated as part of the National Bioresource Project (Japan). $P^{snap\text{-}25}$*:gfp* was a gift from Dr Junho Lee (Seoul National

[1]Department of Biochemistry, College of Science, Yonsei University, Seoul 120-749, Korea. [2]School of Life Sciences and Biotechnology, Korea University, Seoul 136-701, Korea. [3]Institute of Molecular Biology, University of Zurich, 8057 Zurich, Switzerland.

*These authors contributed equally to this work
†Author for correspondence (e-mail: kooh@yonsei.ac.kr)

Accepted 13 July 2006

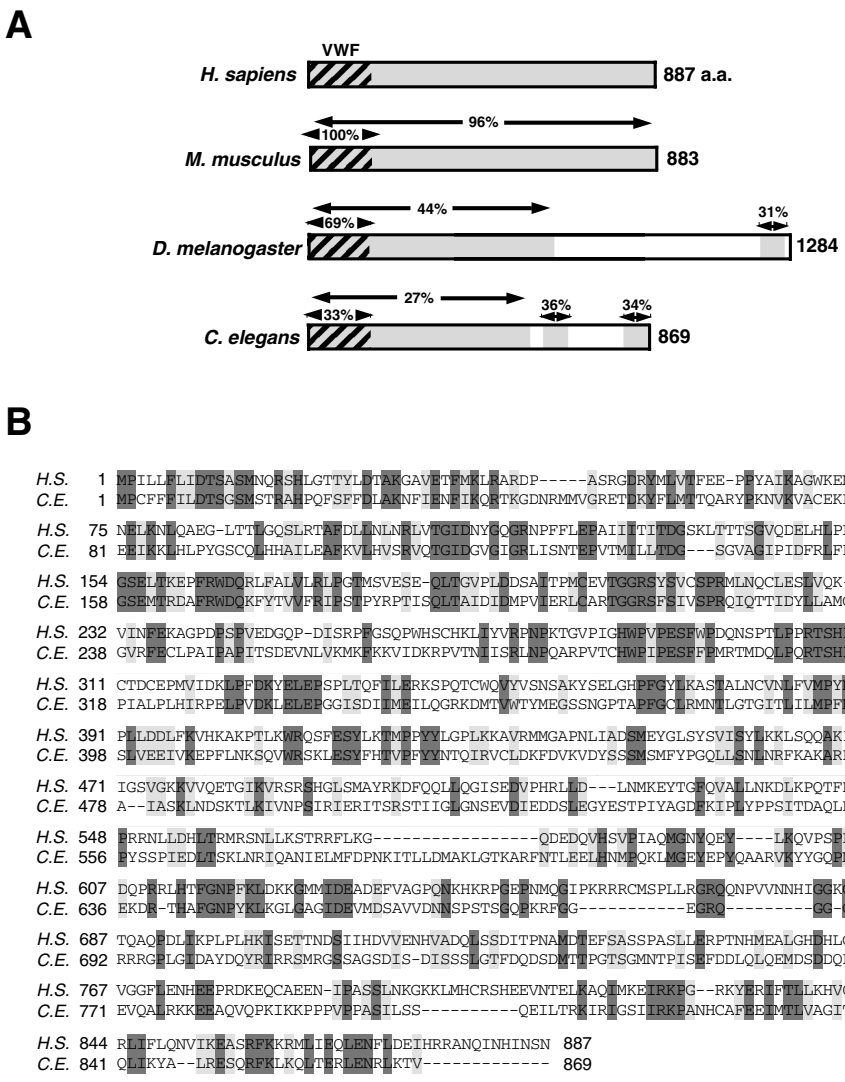

Fig. 1. Evolutionary conservation of DICE1. (**A**) Amino acid sequence alignment of DICE1 homologs in *C. elegans*, human, mouse and fly. The striped boxes represent von Willebrand factor type A motifs, and the gray and white boxes are homologous and non-conserved regions, respectively. The percentages refer to identical amino acids in the human homolog and the other proteins. (**B**) The amino acid sequences of the human and *C. elegans* DICE1 homologs were compared using the Vector NTI Advance program (Invitrogen). Dark and light gray backgrounds of letters signify identical and similar amino acids, respectively.

University, Seoul, Korea) and *unc-15(paramyocin)::gfp* was obtained from Dr Hiroaki Kagawa (Okayama University, Japan). The *P*$^{myo\text{-}3}$*::mito::gfp* DNA construct was obtained from Dr Alexander M. Van der Bliek (University of California, Los Angeles, CA, USA), an EST clone of the *dic-1* gene (yk293c3) from Dr Yuji Kohara (National Institute of Genetics, Japan) and pPD expression vectors from Andrew Fire (Stanford University, CA, USA).

Bacteria-mediated RNAi of *dic-1*

RNAi was performed by feeding *C. elegans* worms with *E. coli* HT115(DE3) cells expressing double-stranded RNA (dsRNA) for the *dic-1* gene (Kamath et al., 2001). The yk293c3 EST clone of *dic-1* (F08B4.1) was digested with *Hin*dIII enzyme, and the resulting 1.6 kb cDNA fragment was cloned into vector pPD129.36(L4440), which contains convergent T7 polymerase promoters separated by a multicloning site. The resulting construct was transformed into *E. coli* HT115(DE3) (Timmons and Fire, 1998). Transformants were grown in LB medium containing 100 μg/ml of ampicillin for 18 hours and seeded onto NGM plates supplemented with 100 μg/ml of ampicillin and 1 mM isopropyl-thio-β-D-galactoside (IPTG). To examine gonads and mitochondria of adult worms, RNAi was performed from the L1 larval stage. To observe the embryonic phenotypes induced by knockdown of *dic-1*, L4 stage worms were grown on NGM plates covered with *E. coli* cells producing dsRNA of *dic-1* for 24 hours. Adult worms were transferred to new NGM plates, allowed to lay eggs for 6 hours, and then removed. Embryo hatching was scored 24 hour later.

Outcross of the *dic-1(tm1615)* mutant and rescue of larval arrest by wild type *dic-1*

The *dic-1(tm1615)* heterozygous strain from the National Bioresource Project was outcrossed with N2 strains four times to remove possible unrelated mutations. The mutant harbors a deletion of 588 bp, corresponding to nucleotides 32905 to 33492 in the cosmid clone F08B4 (Fig. 7). Primers used for PCR reactions to probe the deletion were as follows: outer sense, 5′-GGTATTTCGTATTCCATCCACTCC; outer antisense, 5′-CCTTGAAATCTCCTGCATAAATAGG; inner sense, 5′-ACGAAGCTTCTCAATTGTATCACC; and inner antisense, 5′-CCTCAATATCAACTTCACTGTTTCC. To observe the phenotypes of *dic-1(tm1615)* homozygotes, worms were mounted on slides overlaid with 2% agar and observed with Nomarski optics (DMR HC, Leica). *C. elegans dic-1(tm1615) IV/nT1[qIs51] (IV;V)* heterozygotes were generated by crossing *dic-1(tm1615)* heterozygotes with *nT1[qIs51]*/+ males that were the progeny of a cross between *elo-5(ok683)/nT1[qIs51]* hermaphrodites and N2 males

To test for rescue of the homozygotes by the wild-type gene, a DNA fragment containing wild-type *dic-1* gene from 1.9 kb upstream of the start codon to 1.3 kb downstream of the stop codon was amplified from the F08B4 cosmid genomic DNA clone using the Expand Long Template PCR system (Roche). The amplified DNA fragment was cloned into pCR2.1-TOPO vector (Invitrogen) and the recombinant plasmid DNA (2 μg/ml) was microinjected into the gonads of young adult *C. elegans dic-1(tm1615)/nT1[qIs51]* heterozygotes, together with pRF4 plasmid DNA (100 μg/ml) (Krammer et al., 1990). Heterozygous transgenic worms in the F1 progeny were selected and maintained by observing their rolling

(*rol-6*) and *gfp*-positive phenotypes. Rescue of homozygotes by the wild-type *dic-1* gene was judged by scoring *gfp*-negative rollers reaching the adult stage.

To test whether human DICE1 can replace *C. elegans* DIC-1, a 2.7 kb coding region of human *DICE1* gene was amplified from cDNA clone MGC:48751 (Invitrogen) as described above. The amplified cDNA fragment was cloned into pPD49.78 plasmid with an *hsp-16.2* promoter, followed by microinjection into the gonads of *dic-1(tm1615)/nT1[qIs51]* heterozygotes together with pRF4 plasmid DNA. Rolling heterozygotes were allowed to lay embryos and the progeny were treated at the L1 stage by heat shock at 30°C for 1 hour to induce expression of the human *DICE1* in their extra-chromosomal arrays. The rescue of homozygotes by human DICE1 was judged as above, by scoring *gfp*-negative rollers reaching the adult stage. As a positive control for the rescue, the coding region of *C. elegans* DIC-1 was amplified from the yk293c3 cDNA clone and cloned into pPD49.78. A transgenic line was obtained and the rescue of larval arrest in homozygotes was confirmed after heat shock induction of the *dic-1* cDNA expression.

GFP-tagged DIC-1 expression in *C. elegans*

To visualize the subcellular location of *C. elegans* DIC-1, the protein was fused with GFP and expressed under the control of either the *hsp-16.2* or *myo-3* promoter. The 2.6 kb cDNA fragment of *dic-1* was cloned into pPD118.26 or pPD114.98, and transgenic lines were generated by microinjecting recombinant plasmid DNA (20 μg/ml) together with pRF4 plasmid DNA (50 μg/ml) into adult N2 worms. Adult worms of the transgenic line $P^{hsp\text{-}16.2}$*::dic-1::gfp* were heat shocked at 30°C for 1 hour and GFP expression was observed in the progeny embryos 3 hours later.

Counts of apoptotic cells

Cell corpses in the germ line were counted by mounting worms in a drop of M9 solution and observing the gonads with Nomarski optics (DMR HC, Leica). Because corpses are cellularized and more refractive than normal cells, they can be readily identified under high magnification at the late pachytene stage. We observed cell corpses in embryos after mounting 380 cell or bean cell stage embryos on slides coated with 0.1% poly-L-lysine. We also performed TUNEL staining to detect apoptotic cells in the embryos with an In Situ Cell Death Detection Kit (Roche) according to the manufacturer's instructions. Embryos were freeze-cracked, fixed and transferred to the wells of a polylysine-coated slide. TUNEL reaction mixture (10 μl of enzyme solution and 90 μl of label solution per well) was added to the fixed embryos and they were allowed to incubate in the dark for 2 hours at 37°C in a humidified atmosphere. After washing with PBS, the specimens were stained with DAPI (4,6-diamidino-2-phenylindole, 1 μg/ml) for 10 minutes and observed with a fluorescence microscope.

Visualizing mitochondria with mitotracker and using a *C. elegans* strain expressing GFP in mitochondria

To stain mitochondria in adult worms, L4 stage worms were transferred to NGM plates containing Mitotracker Red (Molecular Probes, 2 μg/ml) and incubated in the dark at 20°C for 12 hours. They were then transferred to new NGM plates to reduce nonspecific staining. After 10 to 20 minutes, they were mounted on a slide overlaid with 2% agar and observed with a fluorescence microscope. The $P^{myo\text{-}3}$*::mitochondrial signal sequence::gfp* transgenic line, in which muscle cell mitochondria are marked by GFP, was used to observe changes in mitochondrial morphology after *dic-1* RNA*i*.

Antibody preparation

The yk293c3 EST clone of *dic-1* (F08B4.1) was digested with *Eco*RI, and the resulting 1.3 kb cDNA fragment (amino acid residues 143-570) was cloned into pGEX-5X-2 expression vector (Amersham Biosciences). *E. coli* BL21 cells harboring pGEX-5X-2/*dic-1* were cultured at 37°C to an optical density at 600 nm of 0.6, at which time IPTG was added to 1 mM. After incubation for 4 hours, the cells were harvested and sonicated in 10 ml of lysis solution (200 mM Tris-Cl, pH 8.0, 500 mM NaCl, 0.1 mM EDTA,

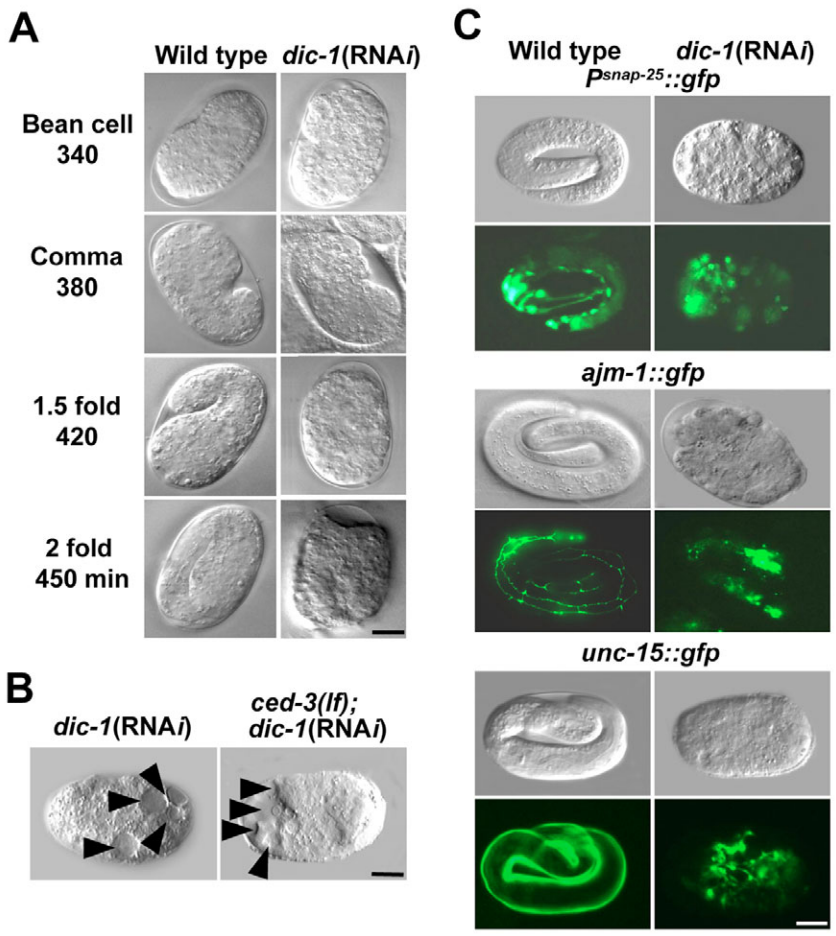

Fig. 2. Abnormal morphogenesis and tissue-specific gene expression in *dic-1* (RNA*i*) embryos. RNA interference was carried out from the L4 stage by feeding bacteria producing double-stranded RNA. (**A**) Time lapse microscopy of embryonic development using Nomarski optics. Developmental stage and time post fertilization (in minutes) are indicated for each wild-type embryo. *dic-1*(RNA*i*) embryos laid at the same time as the wild-type embryos were arrested after the bean cell stage but before the comma stage. (**B**) Embryos obtained after RNA*i* of *dic-1* in wild-type N2 and *ced-3(n717)*, after longer incubation than in A. Cavities are marked with arrowheads. (**C**) Wild-type embryos at the threefold stage and *dic-1*(RNA*i*) embryos at the same time post fertilization, showing $P^{snap\text{-}25}$*::gfp* expression in neurons, *ajm-1::gfp* expression in the junctions of intestinal cells and *unc-15::gfp* expression in muscle cells. Scale bars: 10 μm.

0.1% Triton X-100, 0.4 mM PMSF). The lysate was spun in a microcentrifuge at 11,000 ***g*** for 5 minutes and the supernatant electrophoresed on an 8% SDS polyacrylamide gel. The gel piece containing the fusion protein was excised, crushed in PBS, mixed with Freund's adjuvant and injected into Balb/c mice four times at 10 day intervals (200 μg of protein per injection).

Immunostaining

C. elegans embryos were immunostained by a slightly modified version of the procedure of Crittenden and Kimble (Crittenden and Kimble, 1999). Embryos were freeze-cracked, fixed, incubated with polyclonal mouse antiserum against DIC-1 (1:50 dilution), followed by FITC-conjugated goat anti-mouse immunoglobulin G (1:1000 dilution, Molecular Probes). After staining with DAPI (1 μg/ml), the specimens were observed with a fluorescence microscope. For staining, gonads were extruded from decapitated adult worms, fixed in 3% paraformaldehyde and 0.1 M K_2HPO_4 (pH 7.2) for 1 hour, post-fixed with cold methanol, and incubated with primary and secondary antibodies as described by Jones et al. (Jones et al., 1996). To double-stain DIC-1 and cytochrome c oxidase, gonads were incubated successively with polyclonal mouse antiserum against DIC-1, FITC-conjugated goat anti mouse immunoglobulin G, and Alex Fluor 594-conjugated mouse immunoglobulin G against bovine cytochrome c oxidase subunit 1 (Molecular Probes).

Cryo-electron microscopy

C. elegans worms were plunged into liquid propane at 180°C. The frozen samples were then transferred to substitution medium (acetone) and freeze-substituted at 80°C for 72 hours, after which the temperature was raised to 40°C at a rate of 6°C hr^{-1}. The samples were washed three times in pre-cooled pure acetone over a period of 1 hour, and then infiltrated with a spur resin (EMS). Infiltration was performed with acetone/resin mixtures (v/v) of 3:1, 1:1 and 1:3 for 1 hour each and with the pure resin for 3 hours. The resin was polymerized at 60°C for 48 hours. Sections about 60 nm thick were cut horizontal to the plane of the sample using an ultra-microtome (RMC MTXL) and mounted on nickel grids. They were stained with uranyl acetate and lead citrate and viewed at 120 kV with a Technai 12 electron microscope (Philips, Netherlands).

For immunogold labeling, the ultra-thin sections on nickel grids were etched with 10% hydrogen peroxide for 30 minutes, rinsed in deionized water and floated on 0.56 mM sodium metaperiodate. They were then rinsed with deionized water and floated for 1 hour in PBS containing 1% bovine serum albumin (PBS-BSA), followed by overnight incubation at 4°C in anti-mouse DIC-1 diluted to 1:200 with PBS-BSA. After rinsing several times with PBS-BSA, they were floated for 1 hour in anti-mouse IgG conjugated to 10 nm gold particles (British Biocell International) diluted to 1:50 with PBS-BSA. The gold-labeled sections were rinsed successively with PBS, PBST (containing 1% Triton X-100) and deionized water, air dried, stained and examined as above by electron microscopy.

RESULTS

dic-1(RNA*i*) embryos are defective in morphogenesis, and form cell cavities

A *C. elegans* DICE1 homolog (DIC-1) is encoded by the F08B4.1 open reading frame (Wormbase, http://www.wormbase.org) and has about 30% identity in its N-terminal, central and C-terminal domains with the corresponding regions of the human homolog, as depicted in Fig. 1. In order to determine the function of DIC-1 in *C. elegans* (DIC-1) during *C. elegans* development, we used RNA interference (RNA*i*) from the L1 or L4 stage. This was accomplished by feeding *C. elegans* worms with *E. coli* cells expressing the cognate double-stranded RNA (dsRNA). RNA interference from the L4 stage resulted in complete lethality of progeny embryos. Time-lapse microscopy using Nomarski optics showed that embryogenesis was normal at the early stage in the *dic-*

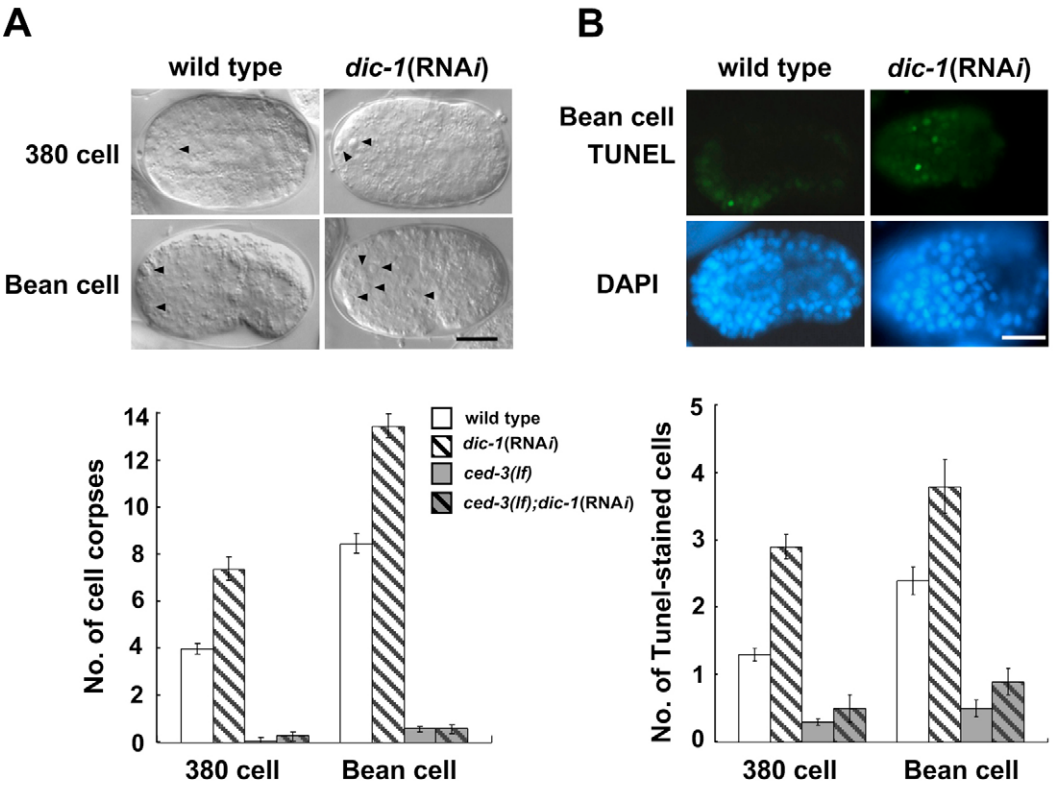

Fig. 3. Increased apoptosis in *dic-1*(RNA*i*) embryos. (**A**) Apoptotic cell corpses (arrowheads) were counted in 380 cell or bean cell stage embryos of wild type N2 strain with or without *dic-1* knockdown. This procedure was repeated with *ced-3(n717)* strain. (**B**) TUNEL-positive cells in wild-type and *dic-1*(RNA*i*) embryos were scored with a fluorescence microscope at the same embryonic stages as in A. Scale bars: 10 μm. Error bars indicate standard errors of the mean (s.e.m.).

1(RNA*i*) strain, whereas it was abnormal from the bean cell stage (Fig. 2A). Even after prolonged incubation, *dic-1*(RNA*i*) embryos never reached the normal comma stage. In addition to their blocked morphogenesis, they contained cell cavities after longer incubation, as shown in Fig. 2B. The formation of these cavities was independent of *ced-3*, suggesting that they were not generated by the major *C. elegans* apoptosis pathway.

We probed tissue-specific morphogenesis using the transgenic strains $P^{snap\text{-}25}$*::gfp*, *ajm-1::gfp* and *unc-15(paramyocin)::gfp*, which express GFP in neurons, in the adherens junctions of pharynx, intestine and hypodermis, and in muscle cells, respectively (Fig. 2C). SNAP-25 is a component of synaptosomes expressed in *C. elegans* neurons (Hwang and Lee, 2003). Fig. 2C illustrates tissue-specific gene expression in wild-type (threefold) and *dic-1*(RNA*i*) embryos at the same time post fertilization, showing similar overall intensity of GFP fluorescence. Although the *dic-1*(RNA*i*) embryos did not pass the comma stage morphologically, the extent of GFP expression suggests that tissue-specific differentiation progressed further; however, the differentiated cells were disorganized, in agreement with the morphogenic abnormalities seen in Fig. 2A.

ced-3-dependent apoptosis is induced in *dic-1*(RNA*i*) embryos and germ line

Although cell cavity formation in *dic-1*(RNA*i*) embryos did not depend on the major apoptosis pathway (Fig. 2B), we tested whether DIC-1 deficiency led to an increased frequency of apoptosis. As *dic-1*(RNA*i*) embryos arrested before the comma stage, apoptotic cells were scored at the 380 cell and bean cell stages either by direct observation of cell corpses under Nomarski optics (Fig. 3A) or after TUNEL staining (Fig. 3B). By both measures, *ced-3(n717)*-dependent apoptosis increased about twofold at the 380-cell stage and 1.6-fold at the comma stage because of knockdown of *dic-1*. Increased apoptosis was also observed in adult gonads upon RNA*i* of *dic-1* from the L4 stage (Fig. 4A). This germline apoptosis was abrogated by the *ced-3(n717)* mutation, as in embryos, and also by the *ced-4(n1162)* mutation, indicating that it was induced via the major apoptosis pathway. It was not affected in the *cep-1(gk138)* background, which rules out DNA damage as the main cause of the apoptosis.

dic-1(RNA*i*) blocks oogenesis and generates cell cavities in the germ line

When RNA*i* of *dic-1* was performed from the L1 stage, various phenotypes appeared, including undersized gonads, inhibition of oogenesis and cavities in the gonad (Fig. 4B). No apparent defects in germline development were observed under Nomarski optics from the mitotic to the pachytene region, apart from some reduction in the number of germ cells. Nevertheless, slightly disturbed immunolocalization was observed in *dic-1*(RNA*i*) gonads for syntaxin 4 in the cytoplasmic membrane, and for porin in the nuclear membrane (S.M.H., unpublished). Although meiotic prophase progression was detected by immunostaining of GLD-1 at the pachytene stage, synapsed chromosomal strands were not as clear in the *dic-1*(RNA*i*) gonad after DAPI staining as in the wild type (S.M.H., unpublished). As in embryos, gonadal DIC-1 deficiency had a marked effect on actively differentiating cells such as late pachytene stage cells and oocytes, but not on rapidly dividing cells. We observed GFP at the rim of the cavities in a transgenic derivative of *dic-1*(RNA*i*) strain expressing annexin V::GFP, which binds to phosphatidylserine in the outer layer of the cytoplasmic membrane of apoptotic and necrotic cells (S. Züllig and T.H.L., unpublished). This suggests that the cavities resulted from apoptotic or necrotic cell death and were not merely vacuoles.

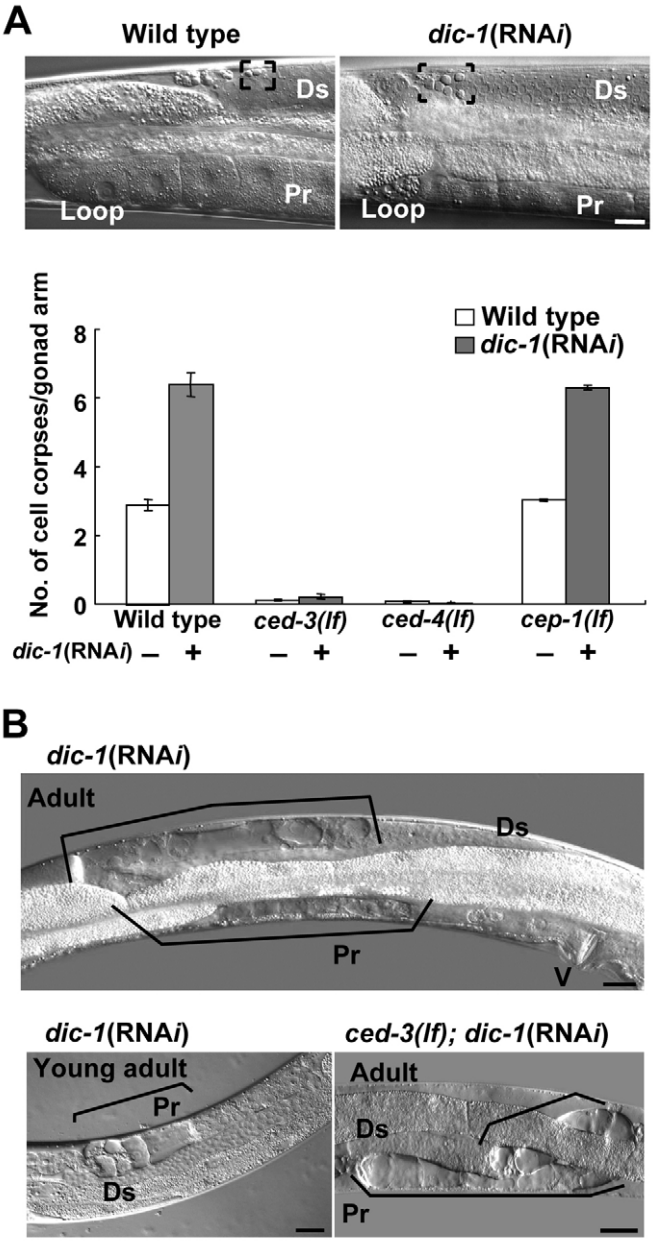

Fig. 4. Increased apoptosis and cell cavity formation in *dic-1*(RNA*i*) gonads. (**A**) Apoptotic cell corpses were counted in the germline with Nomarski optics after feeding *C. elegans* worms with dsRNA encoding *dic-1* for 48 hours from the L4 stage. Germ cell corpses in the loop region of the gonad are indicated by the boxed area. The effects of apoptosis regulators *ced-3(lf)*, *ced-3(n717)*; *ced-4(lf)*, *ced-4(n1162)*; *cep-1(lf)* and *cep-1(gk138)* on the induction of apoptosis by *dic-1*(RNA*i*) are plotted in the graph. Error bars indicate standard errors. (**B**) RNA*i* was performed from the L1 stage and resulted in various phenotypes in the gonad, including undersized gonads, defective oocyte development and cavities. Cavities (brackets) were first observed in the young adult stage gonad but later expanded to the distal tip region of the gonad at the adult stage. *ced-3(lf)*, *ced-3(n717)*. V, vulva; Ds, distal tip region; Pr, proximal region. Scale bars: 25 μm.

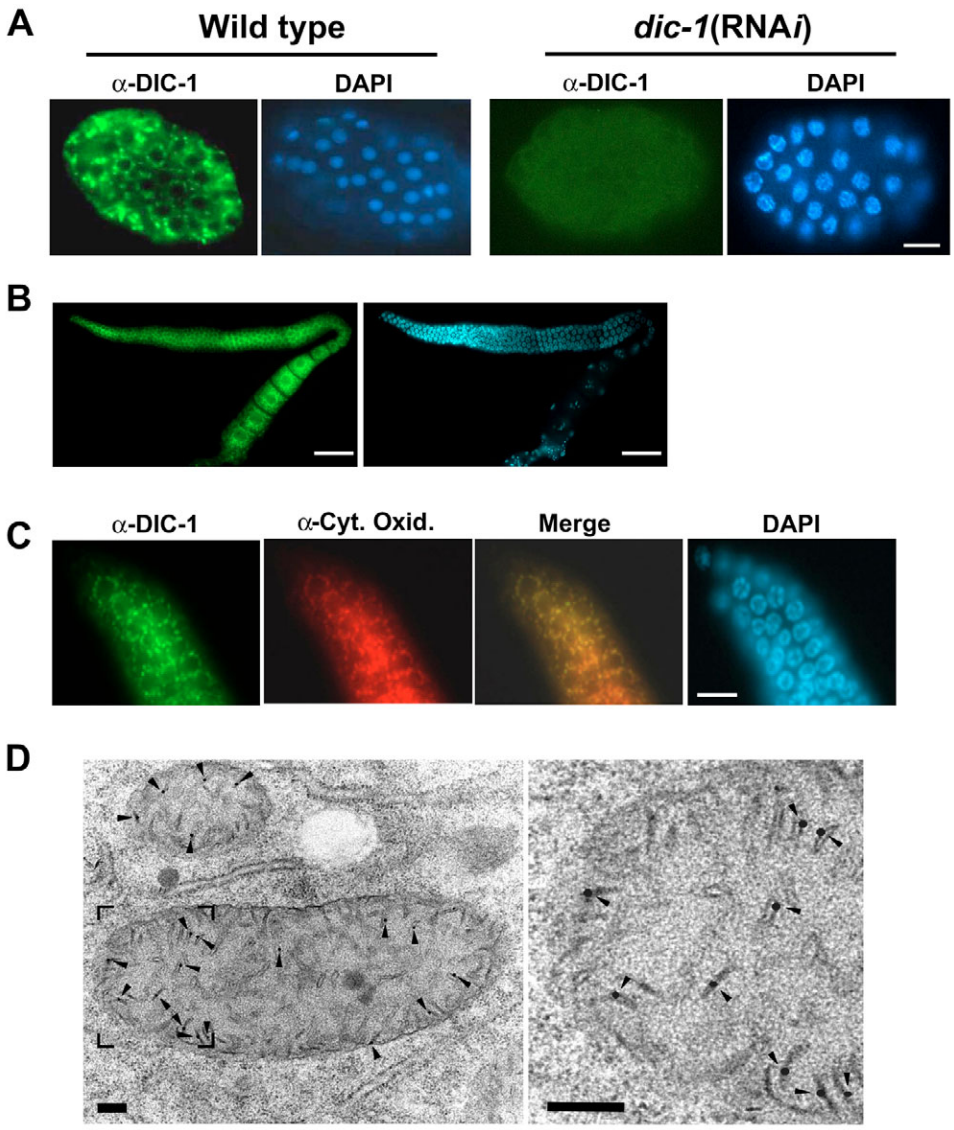

Fig. 5. Immunolocalization of DIC-1 in mitochondria.
(A-C) Immunolocalization of DIC-1 in embryos and germline by fluorescence microscopy. (**A**) Wild-type and *dic-1*(RNA*i*) embryos. (**B**) In wild-type gonads, DIC-1 was restricted to the cytoplasm from the distal tip cells to the oocytes. (**C**) Co-localization of DIC-1 with cytochrome c oxidase subunit 1 within mitotic cells of the gonad. (**D**) Electron micrograph (left) showing immunogold particles (arrowheads) in mitochondria: the bracketed area is enlarged in the right micrograph. Scale bars: 10 μm in A; 50 μm in B; 25 μm in C; 0.2 μm in D.

DIC-1 protein is localized to the mitochondrial inner membrane

When *C. elegans* embryos were reacted with a polyclonal mouse antibody raised against DIC-1, the protein appeared as speckles in the cytoplasm throughout embryogenesis (Fig. 5A). It was present in germ cells and oocytes, and its particulate distribution in the cytoplasm was clearly observed (Fig. 5B,C). At the post-embryonic stage, DIC-1 was present in all somatic cells, although at a lower expression level than in germline cells (S.M.H., unpublished). The speckles of DIC-1 in mitotic germ cells co-localized with anti-cytochrome c oxidase subunit 1 antibody conjugated to Alexa Fluor 594 (Fig. 5C), supporting a mitochondrial location of DIC-1. The mitochondrial localization was confirmed by expressing GFP-tagged DIC-1 under the control of the *hsp16.2* or *myo-3* promoter. The fusion protein localized in the cytoplasm of embryonic cells as foci, as well as in the mitochondria of muscle cells (see Fig. 6), like the GFP fused to a mitochondrial localization signal sequence in Fig. 7B. In agreement with these results, DIC-1 proved to be located in mitochondria by cryo-electron microscopy, more precisely on the inner membrane at cristae (Fig. 5D). The TMpred program (http://www.ch.embnet.org/software/TMPRED_form.html) predicts the presence of two transmembrane regions in DIC-1, encompassing amino acids 129-148 and 377-397, thus supporting the localization in the membrane.

dic-1 knockdown results in morphologically aberrant mitochondria containing numerous vesicles

When wild-type *C. elegans* adults were treated with Mitotracker, which stains active mitochondria, aligned tubular mitochondria were observed parallel to the myofilaments in the muscle cells of wild-type worms (Fig. 7A). By contrast, the muscle cells of *dic-1*(RNA*i*) worms frequently showed disorganized alignment of mitochondria of irregular morphology. The aberrant morphology and disorganized distribution of mitochondria were also observed in transgenic *dic-1*(RNA*i*) worms, in which GFP was targeted to the mitochondrial matrix (Fig. 7B). The more detailed substructure of the morphologically abnormal mitochondria was revealed by cryo-electron microscopy (Fig. 7C). The mitochondria were smaller and packed with numerous vesicles in *dic-1*(RNA*i*) muscle cells, in contrast to the tubular cristae of wild-type worms. The localization of DIC-1 in the inner mitochondrial membrane and the extensive reticular network of

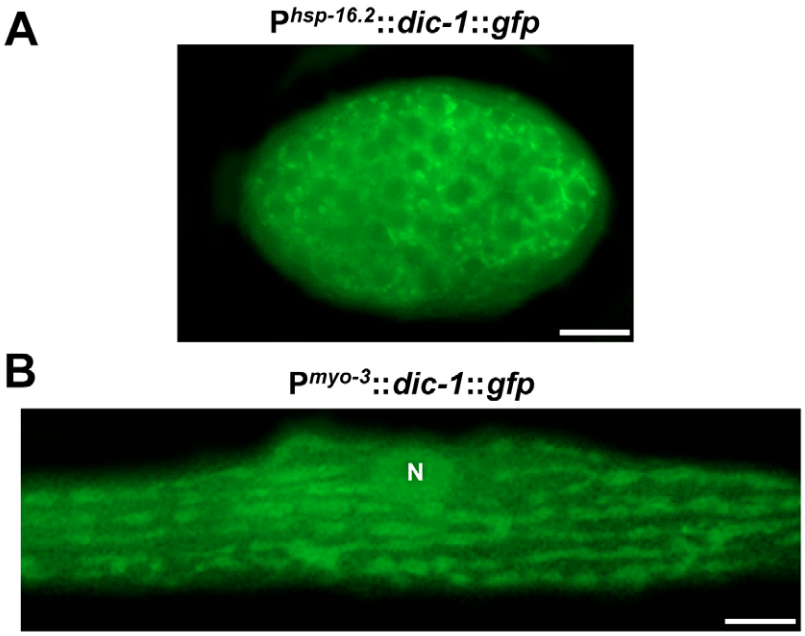

Fig. 6. Subcellular localization of GFP-tagged DIC-1 in embryonic and muscle cells by fluorescence microscopy. (**A**) Expression of GFP-tagged DIC-1 under the control of the *hsp-16.2* promoter was induced by heat shock in N2 worms and spotted expression was observed in the cytoplasm of early embryos. (**B**) GFP-tagged DIC-1 was expressed under the control of the *myo-3* promoter in N2 worms and expression was observed in the mitochondria of body-wall muscle cells. N, nucleus. Scale bars: 10 μm in A; 5 μm in B.

cristae between vesicles in *dic-1*(RNA*i*) mitochondria show that DIC-1 is essential for the formation of normal morphology of cristae/inner membrane.

A *dic-1* deletion mutant is arrested at the L3 larval stage and can be rescued by the wild-type gene

The open reading frame of *dic-1* is predicted by WormBase to consist of 14 exons, but we identified 16 exons when we sequenced the cDNA of the EST clone yk293c3 (Fig. 8A). The *dic-1(tm1615)* strain, obtained from the National Bioresource project for *C. elegans*, was generated by deleting a region of exon 4 and all of exons 5 and 6, and this deletion is very likely to cause premature termination of translation. The homozygous progeny of a heterozygous mother hatched, but they remained arrested at the L3 larval stage for several days, and eventually died. Under Nomarski optics, they were found to have cavities, similar to the cavities in *dic-1*(RNA*i*) embryos and gonads, over much of their bodies (Fig. 8B). In order to determine whether the mutant phenotype could be rescued by the wild-type gene, we generated a *dic-1(tm1615)/nT1[qIs51]* heterozygous strain containing extra-chromosomal arrays of wild-type *dic-1* gene and the *rol-6* gene. Among the progeny of these heterozygotes, 24% (n=554) had a rolling phenotype and 12% of the rollers that reached the adult stage were *dic-1* homozygotes (lacking *nT1[qIs51]* balancer chromosome for pharyngeal GFP expression). On the basis of complete rescue by the wild-type gene, we expect 33% of the adult progeny to be *dic-1* homozygotes. The lower percentage of rescue indicates incomplete rescue, presumably due to mosaicism of the extra-chromosomal array in somatic cells. The rescued adult homozygotes produced almost no viable progeny, probably because the *dic-1* gene in the extra-chromosomal array was silenced in the germ line. By contrast, a mere 0.3% of the non-roller adults (n=580) had a non-fluorescent pharynx, signifying *dic-1* homozygosity.

L3 growth arrest has been observed in mutants defective in mitochondrial proteins (Tsang et al., 2001) and after ethidium bromide treatment, which inhibits mitochondrial DNA replication (Tsang and Lemire, 2002). This L3 arrest is related to the energy requirement for entry into the L4 stage, and the fivefold increase in the number of mitochondrial DNA copies at this time (Tsang and Lemire, 2002). The L3 arrest of *dic-1(tm1615)* homozygotes is yet further evidence that DIC-1 is crucial for mitochondrial activity. When RNA*i* of *dic-1* was performed from the L1 stage, a minor fraction of the worms arrested at the L4 or early adult stage, not at the L3 stage. The incompleteness of RNAi and the later disappearance of zygotic *dic-1* expression may have contributed to the much weaker post-embryonic somatic phenotype of the knockdown strain compared with the knockout mutant.

Expression of human DICE1 does not rescue the larval arrest of *dic-1* homozygotes

In order to determine whether human DICE1 is a functional homolog of *C. elegans* DIC-1, we generated a *dic-1(tm1615)/nT1[qIs51]* heterozygous strains containing extra-chromosomal arrays of human *DICE1* cDNA (or *C. elegans dic-1* cDNA as a positive control) linked to the *hsp-16.2* promoter and the *rol-6* gene. When heterozygotes transformed with *C. elegans dic-1* cDNA were allowed to produce progeny, followed by heat shock at the L1 stage, 11% of the roller progeny (n=682) that reached adulthood were *dic-1* homozygotes. This showed that heat shock-induced *dic-1* cDNA expression rescued the mutant phenotype as effectively as the wild-type *dic-1* gene expression described above. By contrast, none of the adult roller progeny (n=203) was *dic-1* homozygotes when the roller progeny were from heterozygotes transformed with human *DICE1* cDNA. Thus, we were unable to obtain evidence that human DICE1 and *C. elegans* DIC-1 are functionally equivalent. Whether this failure reflects technical limitations with the expression or stability of the human protein in worms, the inability of human DICE1 to interact with essential *C. elegans* partners due to divergence, or a difference in function of the two proteins is not known.

DISCUSSION

DIC-1 is involved in remodeling of the mitochondrial cristae

DIC-1 is expressed ubiquitously as cytoplasmic speckles, and is at a somewhat higher level in oocytes and embryos (Figs 5,6). We narrowed down its location to the mitochondrial inner membrane by immunogold electron microscopy (Fig. 5D). In agreement with this,

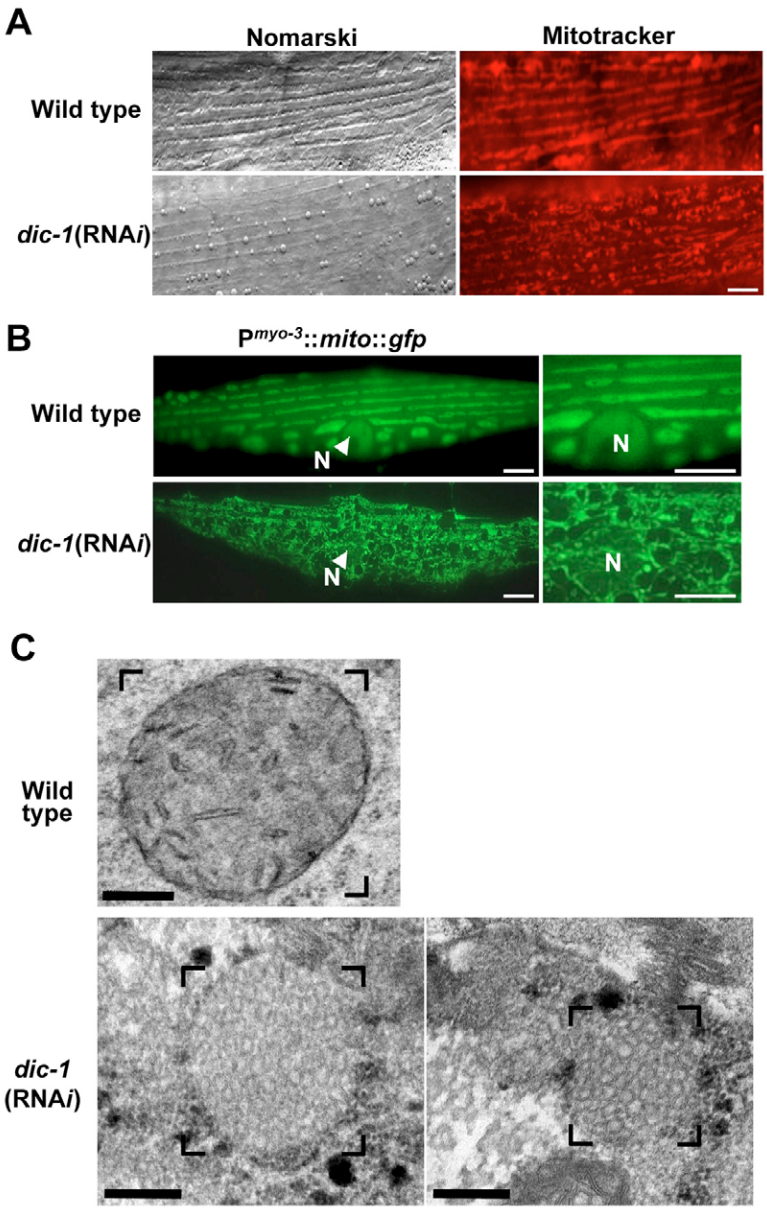

Fig. 7. Disrupted morphology and inner structure of mitochondria in DIC-1(RNA*i*) muscle cells observed by fluorescence microscopy and cryo-electron microscopy. (**A**) The musculature of *dic-1*(RNA*i*) worms shows abnormal morphology of active mitochondria stained with Mitotracker Red. (**B**) The mitochondrial matrix visualized with a mitochondrial matrix-targeting sequence::GFP construct controlled by the *myo-3* promoter. (**C**) Electron micrographs of mitochondria (enclosed by brackets) in wild-type and *dic-1*(RNA*i*) muscle cells. Scale bars: 10 μm in A; 5 μm in B; 0.2 μm in C.

dic-1(RNA*i*) mitochondria had an irregular morphology and disorganized distribution, and contained numerous vesicles in the inner compartment (Fig. 7). Similar structures with reticular cristae or intra-mitochondrial vesicles have been observed in the mitochondria of other species deficient in a mitochondrial fusion protein or overexpressing a fission protein (Griparic et al., 2004; Messerschmitt et al., 2003; Olichon et al., 2003). Fusion and fission of mitochondria occurs dynamically in the cell, via fusion and fission of its membranes (Pfanner et al., 2004; Youle and Karbowski, 2005). In yeast, Mgm1 in the inner membrane, and Ugo1 and Fzo1 in the outer membrane are involved in the fusion process (Pfanner et al., 2004; Wong et al., 2003). Interestingly, when expression of the mammalian homolog of Mgm1, OPA1, was reduced in HeLa cells by siRNA, reticular cristae were formed (Griparic et al., 2004; Olichon et al., 2003). *S. cerevisiae* Mdm33 is involved in the opposite process, fission of the mitochondrial inner membrane, and its overexpression leads to inner vesicle formation, as in DIC-1 deficiency, and to partitioning of the matrix by membrane septa (Messerschmitt et al., 2003).

In addition to causing the formation of reticular cristae, downregulation of OPA1 in HeLa cells induced apoptosis (Lee et al., 2004; Olichon et al., 2003), implying a functional similarity between DIC-1 and OPA1. Nevertheless, knockdown of EAT-3, a *C. elegans* homolog of human OPA1 and of yeast Mgm1, resulted in mitochondrial fragmentation (T.H.L., unpublished), unlike the disorganized and interconnected mitochondrial distribution evident in Fig. 7B. It also resulted in a reduced number of morphologically normal but longer cristae in cryo-electron micrographs (J.Y.M., unpublished). Therefore, DIC-1 is not likely to be involved in fusion of the inner mitochondrial membrane. When FIS1 or DRP1, both of which are involved in fission of the mitochondrial outer membrane, was knocked down in HeLa cells, the mitochondria became elongated and apoptosis was reduced (Lee et al., 2004). The differences between these phenotypic effects and those due to DIC-1 deficiency exclude the possibility that DIC-1 participates in fission of the mitochondrial membrane. Besides fusion and fission proteins, such proteins as mitofilin and e and g subunits of mitochondrial

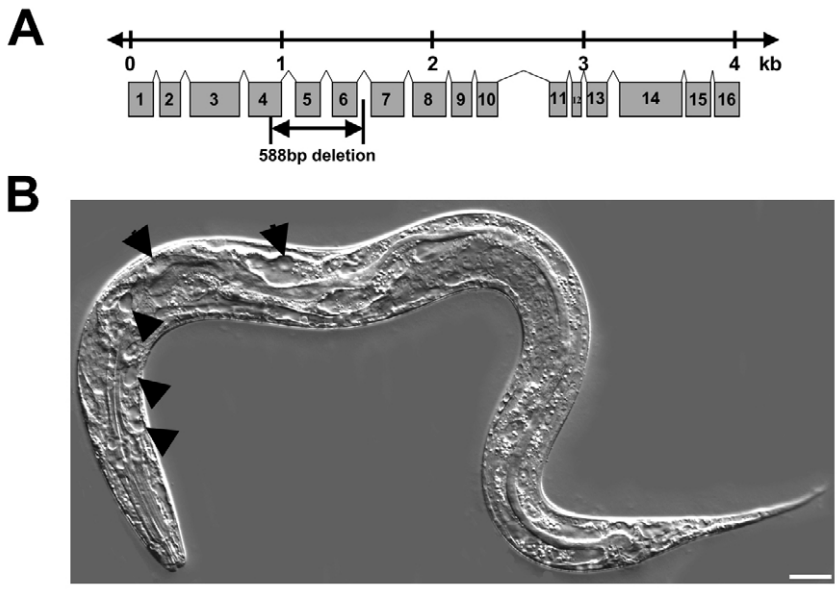

Fig. 8. L3 stage growth arrest of *dic-1(tm1615)*. (**A**) Schematic representation of the *dic-1* gene and the region deleted in the *dic-1(tm1615)* mutation. (**B**) A *dic-1(tm1615)* L3 larva with cavities in all tissues observed with Nomarski optics. Cavities are marked with arrowheads. Scale bar: 50 μm.

ATP synthase control cristae/inner membrane morphology. In mitochondria of HeLa cells deficient in mitofilin, which normally forms a large multimeric protein complex in the intermembrane space, concentrically packed inner membranes were interconnected at numerous sites (John et al., 2005). This 'onion-like' structure was also induced in *S. cerevisiae* cells by decreased expression of e or g subunit of the ATP synthase, both of which are involved not in ATP synthesis but in the oligomerization of the ATP synthase (Arselin et al., 2004). Like mitofilin and the ATP synthase e and g subunits, DIC-1 is thought to be involved rather in remodeling (as a comprehensive term) of the mitochondrial cristae/inner membrane, not in its fusion/fission.

DIC-1 is more crucial at the differentiation stages of oogenesis and embryogenesis

RNA interference of *dic-1* led to *ced-3*-mediated induction of apoptosis in the gonad and embryos. Cell cavities were also generated, but their formation was not dependent on *ced-3*, suggesting that they were generated by necrosis or a minor apoptosis pathway. Cavities were also found in somatic tissues during larval development of the *dic-1(tm1615)* mutant. It is intriguing that similar vacuolar structures were observed throughout the body of a transgenic line overexpressing mutated forms of NUO-1 (NADH- and FMN-binding subunit of complex 1 of the respiratory chain) (Grad and Lemire, 2004). Apoptosis caused by deficiency of *dic-1* was observed at late pachytene and mid-embryonic stages, the developmental stages in which physiological apoptosis normally occurs. Cavity formation was observed at the same or similar stages of germline development and embryogenesis, suggesting a crucial role for DIC-1 at these stages. During the late pachytene/oogenic and the mid-embryonic stages, cells undergo active differentiation to form oocytes and specific tissues, respectively. Efficient mitochondrial activity is probably more crucial in these differentiating cells than in actively dividing cells, as has been observed in a *dif-1* mutant (Ahringer, 1995). DIF-1 is a homolog of mitochondrial carrier proteins involved in solute transport through the inner mitochondrial membrane and is essential during a 3-hour period of active embryonic morphogenesis.

Human DICE1 differs in function and location from its *C. elegans* homolog

In summary, the DICE1 homolog in *C. elegans* is essential for normal mitochondrial morphology and function, and its deficiency induces apoptosis and inhibits development at a number of stages. The major differences between *C. elegans* and mammalian DICE1 homologs are in their subcellular locations and effects on cell proliferation. Although the *C. elegans* protein localizes to mitochondria, the human and mouse homologs localize to nuclei (Hoff et al., 1998; Wieland et al., 2001). When their amino acid sequences were analyzed using the pTARGET program (http://bioinformatics.albany.edu/~ptarget/), *C. elegans* and human DICE1 are predicted to localize in mitochondria at the confidence levels of 93.9% and 75.1%, respectively. However, nuclear localization is predicted for both of the proteins by the pSORT program (http://psort.ims.u-tokyo.ac.jp/) at the probabilities of 73.9% (in *C. elegans*) and 82.6% (in humans). In agreement with this prediction, bipartite nuclear targeting sequences are identified by the PROSITE program (http://www.expasy.org./prosite/) in *C. elegans* (amino acids 677-693 and 693-709) and human DICE1 (amino acids 643-659). Although an exclusive localization of DIC-1 in mitochondria has been observed in this study, it is possible that it translocates to the nucleus under certain conditions. Recently, p53 was found to translocate to mitochondria, as well as to nuclei upon activation by DNA damage or oxidative stress, and it was localized in the matrix and outer membrane of the mitochondria (Chipuk et al., 2004; Zhao et al., 2005).

In addition to the difference in subcellular localization, the *C. elegans* and mammalian DICE1 homologs have distinct effects on cell proliferation and differentiation. The *C. elegans* protein has an anti-apoptotic role and is more important in differentiating cells than in actively dividing ones, in contrast to the role of its mammalian homologs as suppressors of cell proliferation (Hoff et al., 1998; Wieland et al., 2004). When *dic-1(tm1615)* heterozygotes were transformed with a human *DICE1* cDNA under the control of the *C. elegans hsp-16.2* promoter and expression was induced by heat shock at the L1 stage, no rescue of L3 larval arrest was observed in the homozygous *dic-1(tm1615)* progeny. This was probably due to differences in the subcellular location and function of the human homolog and *C. elegans* DIC-1. However, it is also

possible that a low level expression of the human *DICE1* cDNA or instability of the expressed protein could have caused the failure. Human DICE1 was recently reported to be a component of the integrator complex involved in small nuclear RNA processing (Baillat et al., 2005), in agreement with its nuclear localization. Nonetheless, the level of DICE1 mRNA was found to be higher in dominant follicle cells of cow ovaries than in the subordinate follicle cells that subsequently underwent apoptosis (Evans et al., 2004). This result, obtained with cDNA microarrays, suggests an anti-apoptotic role for DICE1 in cows, as observed for its *C. elegans* homolog in the present study. In summary, *C. elegans* DIC-1 plays a crucial role in the formation of normal morphology of mitochondrial cristae/inner membrane, unlike the mammalian homologs that localize in nuclei and are involved in the suppression of cell proliferation. Our results on the *C. elegans* DIC-1 suggest that a re-evaluation and further investigation on mammalian DICE1 may elucidate its multiple functions and/or very complex intracellular dynamics.

C. elegans strains N2, *ced-1(e1735)*, *ced-3(n717)*, *ced-4(n1162)*, *cep-1(gk138)*, *elo-5(ok683)/nT1[qls51]* and *ajm-1::gfp(strain SU93)* were obtained from the *C. elegans* Genetics Center (St Paul, MN, USA), which is supported by the National Center for Research Resources. The *dic-1(tm1615)* strain was kindly generated by the National Bioresource Project (Japan) at our request. We thank Dr Junho Lee (Seoul National University, Seoul, Korea) for $P^{snap\text{-}25}$*:gfp*, Dr Hiroaki Kagawa (Okayama University, Japan) for *unc-15::gfp*, Dr Alexander M. Van der Bliek (University of California, Los Angeles, USA) for the $P^{myo\text{-}3}$*::mito::gfp* DNA construct, Dr Yuji Kohara (National Institute of Genetics, Japan) for the yk293c3 clone of *dic-1*, Dr Alan Coulson (Sanger Center, UK) for the F08B4 clone and Andrew Fire (Stanford University) for pPD expression vectors. Suk Huh (Yonsei University, Korea) made a few plasmid constructs for the phenotype rescue of *dic-1* homozygotes. This work was supported by a Molecular and Cellular BioDiscovery Research Program grant (M1-0311-00-0070) from the Ministry of Science and Technology (to H.S.K.), and also by grants from the Swiss National Science foundation, the Ernst Hadorn Foundation and the Josef Steiner Foundation (to M.O.H.).

References

Ahringer, J. (1995). Embryonic tissue differentiation in *Caenorhabditis elegans* requires *dif-1*, a gene homologous to mitochondrial solute carriers. *EMBO J.* **14**, 2307-2316.

Arselin, G., Vaillier, J., Salin, B., Schaeffer, J., Giraud, M.-F., Dautant, A., Brèthes, D. and Velours, J. (2004). The modulation in subunits e and g amounts of yeast ATP synthase modifies mitochondrial cristae morphology. *J. Biol. Chem.* **279**, 40392-40399.

Baillat, D., Hakimi, M.-A., Näär, A. M., Shilatifard, A., Cooch, N. and Shiekhattar, R. (2005). Integrator, a multiprotein mediator of small nuclear RNA processing, associates with the C-terminal repeat of RNA polymerase II. *Cell* **123**, 265-276.

Chipuk, J. E., Kuwana, T., Bouchier-Hayes, L., Droin, N. M., Newmeyer, D. D., Schuler, M. and Green, D. R. (2004). Direct activation of Bax by p53 mediates mitochondrial membrane permeabilization and apoptosis. *Science* **303**, 1010-1014.

Colombatti, A. and Bonaldo, P. (1991). The superfamily of proteins with von Willebrand factor type A-like domains: one theme common to components of extracellular matrix, hemostasis, cellular adhesion, and defense mechanisms. *Blood* **77**, 2305-2315.

Crittenden, S. L. and Kimble, J. (1999). Confocal methods for *Caenorhabditis elegans*. *Methods Mol. Biol.* **122**, 141-151.

Evans, A. C. O., Ireland, J. L. H., Winn, M. E., Lonergan, P., Smith, G. W., Coussens, P. M. and Ireland, J. J. (2004). Identification of genes involved in apoptosis and dominant follicle development during follicular waves in cattle. *Biol. Reprod.* **70**, 1475-1484.

Grad, L. I. and Lemire, B. D. (2004). Mitochondrial complex I mutations in *Caenorhabditis elegans* produce cytochrome c oxidase deficiency, oxidative stress and vitamin-responsive lactic acidosis. *Hum. Mol. Genet.* **13**, 303-314.

Griparic, L., van der Wel, N. N., Orozco, I. J., Peters, P. and van der Bliek, A. M. (2004). Loss of the intermembrane space protein Mgm1/OPA1 induces swelling and localized constrictions along the lengths of mitochondria. *J. Biol. Chem.* **279**, 18792-18798.

Hoff, H. B., 3rd, Tresini, M., Li, S. and Sell, C. (1998). DBI-1, a novel gene related to the notch family, modulates mitogenic response to insulin-like growth factor 1. *Exp. Cell Res.* **238**, 359-370.

Hwang, S. B. and Lee, J. (2003). Neuron cell type-specific SNAP-25 expression driven by multiple regulatory elements in the nematode *Caenorhabditis elegans*. *J. Mol. Biol.* **333**, 237-247.

John, G. B., Shang, Y., Li, L., Renken, C., Mannella, C. A., Selker, J. M. L., Rangell, L., Bennett, M. J. and Zha, J. (2005). The mitochondrial inner membrane protein mitofilin controls cristae morphology. *Mol. Biol. Cell* **16**, 1543-1554.

Jones, A. R., Francis, R. and Schedl, T. (1996). GLD-1, a cytoplasmic protein essential for oocyte differentiation, shows stage- and sex-specific expression during *Caenorhabditis elegans* germline development. *Dev. Biol.* **180**, 165-183.

Kamath, R. S., Martinez-Campos, M., Zipperlen, P., Fraser, A. G. and Ahringer, J. (2001). Effectiveness of specific RNA-mediated interference through ingested double-stranded RNA in *Caenorhabditis elegans*. *Genome Biol.* **2**, 1-10.

Krammer, J., French, R. P., Park, E. and Johnson, J. J. (1990). The *Caenorhabditis elegans rol-6* gene, which interacts with the *sqt-1* collagen gene to determine organismal morphology, encodes collagen. *Mol. Cell. Biol.* **10**, 2081-2089.

Lee, Y.-J., Jeong, S.-Y., Karbowski, M., Smith, C. L. and Youle, R. J. (2004). Roles of the mammalian and mitochondrial fission and fusion mediators Fis1, Drp1, and Opa1 in apoptosis. *Mol. Biol. Cell* **15**, 5001-5011.

Messerschmitt, M., Jacobs, S., Vogel, F., Fritz, S., Dimmer, K. S., Neupert, W. and Westermann, B. (2003). The inner membrane protein Mdm33 controls mitochondrial morphology in yeast. *J. Cell Biol.* **160**, 553-564.

Olichon, A., Baricault, L., Gas, N., Guillou, E., Valette, A., Belenguer, P. and Lenaers, G. (2003). Loss of OPA1 perturbates the mitochondrial inner membrane structure and integrity, leading to cytochrome c release and apoptosis. *J. Biol. Chem.* **278**, 7743-7746.

Pfanner, N., Wiedemann, N. and Meisinger, C. (2004). Double membrane fusion. *Science* **305**, 1723-1724.

Röpke, A., Buhtz, P., Böhm, M., Seger, J., Wieland, I., Allhoff, E. P. and Wieacker, P. F. (2005). Promoter CpG hypermethylation and downregulation of *DICE1* expression in prostate cancer. *Oncogene* **24**, 6667-6675.

Timmons, L. and Fire, A. (1998). Specific interference by ingested dsRNA. *Nature* **395**, 854.

Tsang, W. Y. and Lemire, B. D. (2002). Mitochondrial genome content is regulated during nematode development. *Biochem. Biophys. Res. Commun.* **291**, 8-16.

Tsang, W. Y., Sayles, L. C., Grad, L. I., Pilgrim, D. B. and Lemire, B. D. (2001). Mitochondrial respiratory chain deficiency in *Caenorhabditis elegans* results in developmental arrest and increased life span. *J. Biol. Chem.* **276**, 32240-32246.

Whittaker, C. A. and Hynes, R. O. (2002). Distribution and evolution of von Willebrand/Integrin A domains: widely dispersed domains with roles in cell adhesion elsewhere. *Mol. Biol. Cell* **13**, 3369-3387.

Wieland, I., Arden, K. C., Michels, D., Klein-Hitpass, L., Bohm, M., Viars, C. S. and Weidle, U. H. (1999). Isolation of DICE1: a gene frequently affected by LOH and downregulated in lung carcinomas. *Oncogene* **18**, 4530-4537.

Wieland, I., Ropke, A., Stumm, M., Sell, C., Weidle, U. H. and Wieacker, P. F. (2001). Molecular characterization of the DICE1 (DDX26) tumor suppressor gene in lung carcinoma cells. *Oncol. Res.* **12**, 491-500.

Wieland, I., Sell, C., Weidle, U. H. and Wieacker, P. (2004). Ectopic expression of DICE1 suppresses tumor cell growth. *Oncol. Rep.* **12**, 207-211.

Wong, E. D., Wagner, J. A., Scott, S. V., Okreglak, V., Holewinske, T. J., Cassidy-Stone, A. and Nunnari, J. (2003). The intramitochondrial dynamin-related GTPase, Mgm1p, is a component of a protein complex that mediates mitochondrial fusion. *J. Cell Biol.* **160**, 303-311.

Youle, R. J. and Karbowski, M. (2005). Mitochondrial fission in apoptosis. *Nat. Rev. Mol. Cell Biol.* **6**, 657-663.

Zhao, Y., Chaiswing, L., Velez, J. M., Batinic-Haberle, I., Colburn, N. H., Oberley, T. D. and St. Clair, D. K. (2005). P53 translocation to mitochondria precedes its nuclear translocation and targets mitochondrial oxidative defense protein-manganese superoxide dismutase. *Cancer Res.* **65**, 3745-3750.